Journal of Power Sources 196 (2011) 2155–2163

Contents lists available at ScienceDirect

Journal of Power Sources

journal homepage: www.elsevier.com/locate/jpowsour

More on the reactivity of olivine $LiFePO_4$ nano-particles with atmosphere at moderate temperature

Jean-Frédéric Martin[a,c], Marine Cuisinier[a], Nicolas Dupré[a,*], Atsuo Yamada[b], Ryoji Kanno[c], Dominique Guyomard[a]

[a] Institut des Matériaux Jean Rouxel (IMN) – CNRS – UMR6502, 2 rue de la Houssinière, B.P. 32229, 44322 Nantes cedex 3, France
[b] Department of Engineering, The University of Tokyo, Building 5-607, 7-3-1 Hongo, Bunkyo-ku, Tokyo 113-8656, Japan
[c] Department of Electronic Chemistry, Interdisciplinary Graduate School of Science and Engineering, Tokyo Institute of Technology, 4259 Nagatsuta, Midori, Yokohama 226-8502, Japan

ARTICLE INFO

Article history:
Received 21 July 2010
Received in revised form
10 September 2010
Accepted 30 September 2010
Available online 8 October 2010

Keywords:
Lithium batteries
$LiFePO_4$
Aging

ABSTRACT

The changes appearing for $LiFePO_4$–C nano-composites exposed to atmosphere at 120 °C have been structurally and chemically examined by the use of TGA, XRD, XPS, Mössbauer, ^{7}Li MAS NMR and electrochemical methods. The results conclude that a highly disordered phase resulting from the aging of $LiFePO_4$ appears on the surface of the grains of the material, is assigned to a phosphate phase and can insert lithium around 2.6 V with poor reversibility. The essential role of water has been investigated and clearly demonstrated. Thus, the aging mechanism occurring in hot humid air is completely different from a simple oxidation as well as from the aging process observed above 150 °C and involves the incorporation of hydroxyl groups. In addition, Fe_2O_3 formation has not been observed for such an aging in mild conditions.

1. Introduction

Triphylite $LiFePO_4$ is currently considered as one of the most promising cathode materials of the new generation of lithium batteries. In this perspective, an extensive research has been carried out concerning its synthesis, its tailoring for Li battery application [1–6], and the understanding of its intercalation mechanism [7–10]. The reduction of the particle size is now understood as a key point to optimize the materials response in terms of capacity and rate capability [8,5,11,12]. Lowering the particle size increases the importance of surface chemistry, including possible parasitic side reactions [13,14]. This aspect, in addition to the intrinsic wider solid-solution domains of nano-particles [11–13,15], becomes crucial when the size drops under 100 nm.

Up to now, only few studies deal with the reaction of synthetic nano-scale $LiFePO_4$ with ambient atmosphere. The essential role of humidity, the appearing of Fe(III) and the reduction of the cell volume of triphylite have been brought forward [16–20] but the reaction mechanism remains unclear. In parallel, aging of natural olivine has been studied by mineralogists. This body of work includes the natural degradation of Fe–Mn based phosphates under soft hydrothermal (low temperature) conditions. Two reaction mechanisms were underlined: lithium extraction with a progressive oxidation of iron and/or manganese following the Quensel–Mason sequence [21,22] describing the transformation of Mn–Fe triphylite into ferrisicklerite and then heterosite:

$$\mathrm{Li(Fe(II)_{1-x}Mn(II)_x)PO_4} \Rightarrow \mathrm{Li_x\square_{1-x}(Fe(III)_{1-x}Mn(II)_x)PO_4} \Rightarrow \mathrm{\square(Fe(III)_{1-x}Mn(III)_x)PO_4} \quad (1)$$

This reaction mechanism has also been proposed by Hatert and Schmid-Beurmann [22] in the case of $LiFePO_4$. The ferrisicklerite keeps the same structure as triphylite with a smaller cell volume. The second possible reaction mechanism emphasizes the role of water with iron oxidation through the incorporation of H_2O or OH^- groups in the structure. Moore [23] proposed two possible reactions:

$$\mathrm{Fe^{II} + H_2O \Rightarrow Fe^{III} + OH^- + 1/2H_2\Uparrow} \quad (2)$$

$$\mathrm{Fe^{II} + OH^- \Rightarrow Fe^{III} + O^{2-} + 1/2H_2\Uparrow} \quad (3)$$

These two reactions are observed for hydrated and hydroxylated iron phosphates and were pointed out by Fransolet [24] in the case of olivine for which they lead, for example, to tavorite-like $LiFe(III)(PO_4)OH$ compound in the case of reaction (2).

More recently, an article by Masquelier and co-workers [19] details the deterioration mechanism of the triphylite in oxidizing atmosphere for temperature from 150 °C up to 700 °C. At their lowest temperature of 150 °C, they conclude on the migration of

* Corresponding author. Tel.: +33 2 40 37 39 33; fax: +33 2 40 37 39 95.
E-mail address: nicolas.dupre@cnrs-imn.fr (N. Dupré).

0378-7753/$ – see front matter © 2010 Elsevier B.V. All rights reserved.
doi:10.1016/j.jpowsour.2010.09.120

iron atoms from the core to the surface of the particles where they react with O_2 to give iron oxide. Fe_2O_3 cannot be however, observed by Mössbauer at this temperature and modifications of local environments using Mössbauer spectroscopy appear from approx. 200 °C. Recent work by our group [20] indicated a different aging mechanism at lower temperature and suggested the formation of an amorphous ferric phosphate after a prolonged contact with 120 °C humid air. Complementary to these previous studies, the work presented here aims to give more precision and to further understand alterations of the material under soft conditions of temperature and humidity, closer to the storage or drying conditions typically used for this material. Combined use of TGA–DSC, Mössbauer, XRD, XPS, and ^{7}Li NMR permits to shed light on the alteration of olivine in atmosphere and to monitor the structural and chemical changes occurring. Finally, electrochemical experiments and EIS aim to grasp the consequences of these modifications. As a conclusion of these studies, a scheme of the most probable aging scenario will be proposed.

2. Experimental

The $LiFePO_4$–C composite was synthesized via the solid-state method developed by Yamada et al. and described in previous papers [5,7]. These composites contain olivine particles, whose size has been evaluated to 80 nm, intimately mixed (but not coated) with 10 wt% Ketjenblack electroconductive carbon. It was possible to avoid any atmosphere contact by the use of a sealed furnace tube, keeping the sample under argon for the transfer to the argon glove box. A similar synthesis without adding electroconductive carbon prior to the 700 °C thermal treatment allows obtaining a pure $LiFePO_4$ carbon-free material.

The TGA–DSC experiments were performed on a SETARAM TG–DSC 111 at 2 °C min^{-1} rate. The drying of air and oxygen were obtained by letting the gas flow through P_2O_5 powder. For wet O_2, the gas was let bubbling in water.

The ^{57}Fe Mössbauer spectra were collected with a ^{57}Co γ-ray source. Velocity and isomer shift calibration were performed using α-Fe as a standard at room temperature.

The XRD diffractograms were obtained on a D8 ADVANCE (BRUKER AXS) apparatus using CuK_α radiation and TOPAS software was used for Rietveld refinement. For amorphous phase quantification, the samples were thoroughly mixed with 15% of reference Si powder (particle size of 500 nm) and Brindley correction was taken into account.

XPS analyses were performed using a KRATOS AXIS ULTRA 165 offering a high-energy resolution. The spectra were recorded in the CEA mode (constant analyzer energy) with an analyzer pass energy of 20 eV to obtain elemental quantification and detailed spectra analysis and to probe 10 nm in depth. The samples were attached on a carbon tape and a charge neutralizer was used to minimize charging effects. Peak assignment and quantification analysis were performed with CASAXPS software.

^{7}Li MAS NMR measurements were carried out at room temperature on a Bruker Avance-500 spectrometer (B_0 = 11.8 T, Larmor frequency ν_0 = 194.369 MHz in ^{7}Li resonance). The measurement procedure refers to a previous work done on $LiNi_{0.5}Mn_{0.5}O_2$ samples in order to visualise diamagnetic lithium on the surface of a paramagnetic material. This method is very useful in the case of $LiFePO_4$ as the XPS signal of lithium is superimposed with an iron peak. Single-pulse MAS spectra were obtained by using a Bruker MAS probe with a cylindrical 4-mm o.d. zirconia rotor. Spinning frequencies up to 14 kHz were utilized. A short single pulse length of 1 μs corresponding to a non-selective $\pi/2$ pulse was used. Recycle time was in the 0.5–60 s range and a spectrometer dead time (preacquisition delay) of 4.5 μs was used before each acquisition.

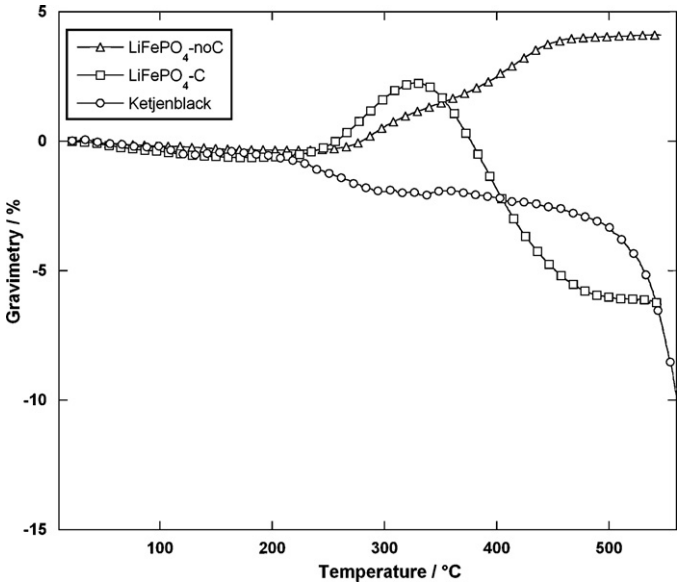

Fig. 1. TGA in ambient air of carbon free $LiFePO_4$ (triangles), 10 wt% carbon–$LiFePO_4$ composite (squares) and Ketjenblack electroconductive carbon (circles). The heating rate is 2 °C min^{-1}.

The isotropic shifts, reported in parts per million, are relative to an external liquid 1 M LiCl aqueous solution set at 0 ppm. The spectra were quantitatively compared via the total integrated intensity of the signal for each sample. All parameters were kept constant for each series of NMR measurements: number of scans, probe tuning process, spinning frequency, etc. The spectra displayed in this work were normalized to the number of scans and the mass of the sample.

Galvanostatic cycling was performed using Swagelok cells and MacPile system at a C/20 rate. A slurry of the electrode powder in n-methyl-pyrolidinone (NMP) was deposited on a 1 cm^2 aluminum disk and then dried under vacuum at 100 °C for 24 h. Electrodes were constituted of 75 wt% of active material, 20 wt% of ketjenblack carbon and 5 wt% poly-vinylidene di-fluoride (PVdF).

Electrochemical impedance spectroscopy (EIS) measurements (from 50 mHz to 200 kHz) were obtained using a VMP/Z apparatus (Bio-logic, France). A home-made Swagelok-type three electrodes cell was used. The negative electrode was made of a disk of lithium metal. The reference electrode consisted of a ring of lithium metal surrounding the working electrode. Measurements have been performed at the end of a 5 h relaxation rest.

3. Results

3.1. Thermogravimetric analyses

TGA experiment under argon on a severely aged sample (30 days at 120 °C), previously published [20], indicated the presence of structural water or hydroxyl group in aged $LiFePO_4$. In order to obtain additional information on the necessary conditions for the aging mechanism to occur, TGA/DSC experiments under various atmospheres were performed on pristine and aged samples. The TGA of $LiFePO_4$–C composite performed in ambient air until 550 °C is presented in Fig. 1. Comparison with the response of pure Ketjenblack carbon and carbon-free olivine allows here separating contributions of olivine and carbon. The carbon free $LiFePO_4$ exhibits a progressive gain of mass between 250 °C and 450 °C corresponding to the oxidation of iron phosphate to iron oxides and $Li_3Fe_2(PO_4)_3$ as shown by Masquelier and co-workers [19] and resulting in a red powder. After a slow weight loss until 300 °C

attributed to water desorption, the carbon reacts with ambient air around 600 °C (see insert in Fig. 1) and quickly disappears. The curve obtained for the $LiFePO_4$–C composite includes an increasing of the mass between 250 °C and 325 °C assigned to the oxidation of $LiFePO_4$ followed by a weight loss between 325 °C and 500 °C due to the departure of the 10 wt% of carbon. This weight loss appears at a slightly lower temperature in the case of the composite. No additional phenomenon is observed. Fig. 2a and b displays the corresponding XRD patterns obtained before the TGA experiment, at the temperature of interest (120 °C) and after the TGA experiment for $LiFePO_4$–C and $LiFePO_4$ respectively. In both cases, no crystallized impurity is detected at 120 °C and only the olivine can be observed. The complete oxidation into $Li_3Fe_2(PO_4)_3$ is also confirmed after the phenomenon observed between 250 °C and 450 °C.

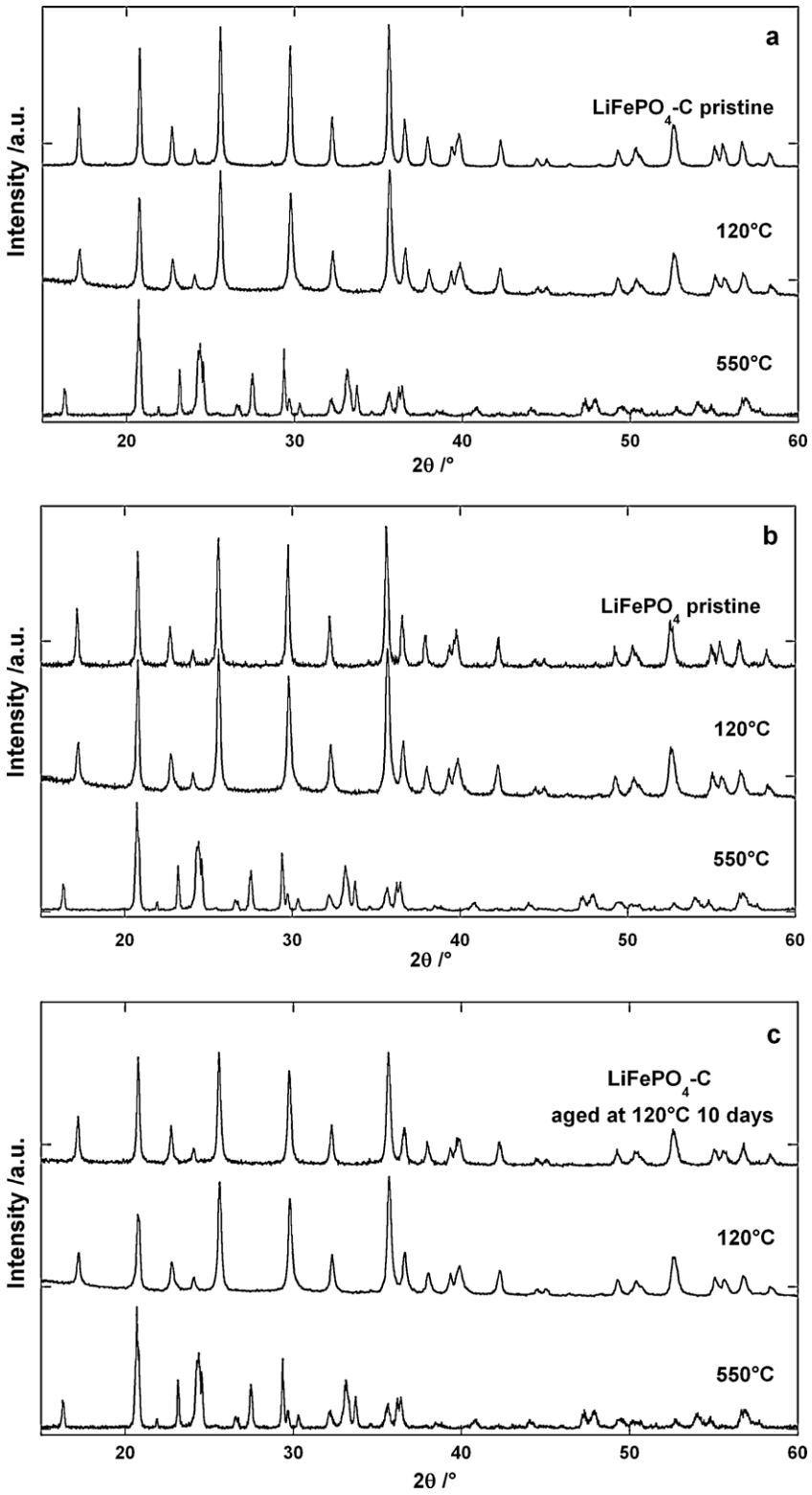

Fig. 2. XRD patterns of $LiFePO_4$–C (a), $LiFePO_4$ (b) and $LiFePO_4$–C aged 10 days at 120 °C (c) pristine, at 120 °C and after the TGA experiments under ambient atmosphere.

Table 1
Lattice parameters extracted from the XRD diagrams obtained for $LiFePO_4$–C samples preserved from atmosphere, exposed at 120 °C, 10 days to ambient atmosphere, dry air and argon and 1 day to CO_2. *x* gives the calculated equivalent missing lithium using a Vegard's law (see Ref. [16]).

Atmosphere treatment	*a* (Å)	*b* (Å)	*c* (Å)	*V* (Å^3)	*x*
No exposure	10.3308(2)	6.0081(1)	4.6944(1)	291.378(6)	0
Ambient atmosphere	10.3100(2)	5.9987(2)	4.6973(2)	290.51(1)	0.041
Dry air	10.3254(3)	6.0054(2)	4.6937(2)	291.05(2)	0.012
CO_2	10.3290(3)	6.0072(2)	4.6936(2)	291.23(2)	0.004
Argon	10.3304(3)	6.0079(1)	4.6937(2)	291.30(2)	0.001

Fig. 3 shows the TGA curves for $LiFePO_4$–C composites for various conditions of storage. The masses of these three samples have been followed during a slow increasing of temperature (2 °C min^{-1}) until 550 °C in ambient atmosphere. The major phenomena, already visible in Fig. 1 in the 250–550 °C range, are reproduced. A similar evolution is also observed by XRD (Fig. 2a and c) for $LiFePO_4$–C and $LiFePO_4$–C aged 10 days at 120 °C i.e. no modification of the XRD pattern observed at 120 °C and complete oxidation into $Li_3Fe_2(PO_4)_3$ after the TGA experiments. Differences between composite samples that have been preserved from atmosphere and samples that have undergone a contact with atmosphere during 10 days at room temperature and at 120 °C can be visualized at lower temperature (see insert of Fig. 3) showing a clear influence of the contact with the atmosphere. Considering that our previous studies [16,20] have demonstrated that the composite undergoes an effect of atmosphere storage at room and low temperature (120 °C), the area localised at the lowest temperature range of the experiment is of the most interest. In this domain, a sample that has never experienced atmosphere contact displays a slight increase of mass around 150 °C. This gain of mass, not visible for an aged sample, can be attributed to the reaction of the preserved olivine sample with ambient atmosphere whereas an aged sample has already sustained this reaction upon storage in atmosphere. Instead, samples exposed to air only display a slight decrease of mass assigned to the departure of adsorbed moisture. The temperature marking the beginning of the weight gain is situated above 100 °C and therefore, this additional phenomenon cannot be assigned to a simple adsorption of water. For this reason, if water is involved in this weight gain, this water must be chemisorbed and reacting with the sample.

Possible reaction of the olivine with CO_2 was ruled out in previous works [13,25]. Here, in addition, we performed additional Rietveld refinements on samples aged under CO_2 atmosphere, which showed negligible variation of cell parameters, indicating therefore a readily negligible alteration due to CO_2 exposure (Table 1). CO_2 can then be removed from the list of potential reagents. Reaction with O_2 and H_2O will be further discussed below. In order to discriminate the species present in the ambient atmosphere and reacting at low temperature with the olivine, TGA experiments under various gases have been performed on $LiFePO_4$–C composite samples preserved from ambient atmosphere except for the few seconds necessary to the setting of the sample in the TGA crucible. The results are displayed in Fig. 4 and include argon, ambient "wet" atmosphere and dried atmosphere curves. The lattice parameters obtained from XRD pattern of olivine exposed 10 days at 120 °C to these gases are gathered in Table 1. Concerning the argon curve, only water departure is noticed and stops at around 325 °C with a total water amount of around 1.1 wt%. This is attributed to the water taken by the material during the preparation of the sample. This important quantity, although the material has spent only few seconds in atmosphere, demonstrates the important interaction between water and the composite. The

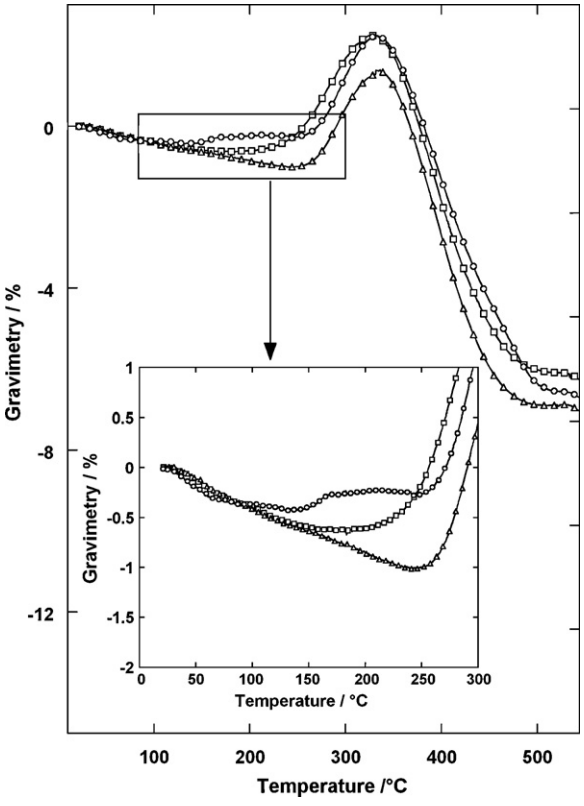

Fig. 3. TGA–DSC curves under ambient atmosphere, obtained for $LiFePO_4$–C composite samples stored in argon (circles), exposed 10 days to ambient atmosphere at R.T. (squares) and at 120 °C (triangles). The heating rate is 2 °C min^{-1}. The insert is a zoom of the low temperature area.

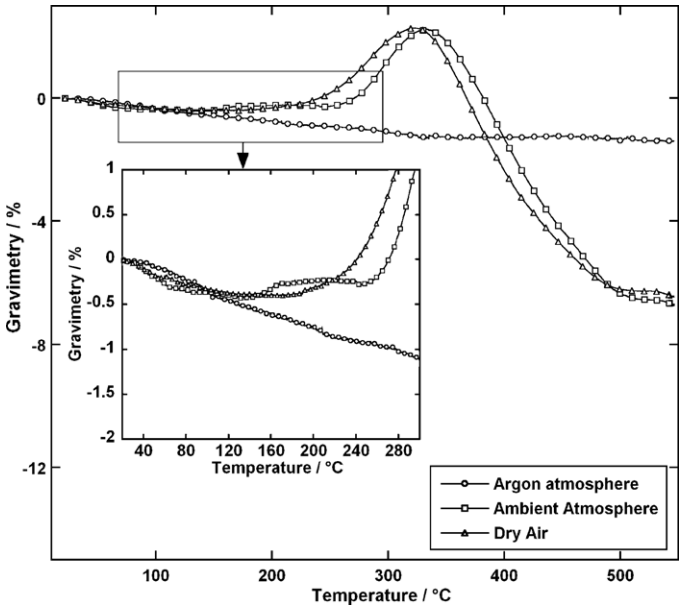

Fig. 4. TGA curves carried out under different gases for $LiFePO_4$–C composite samples preserved from ambient atmosphere. Heating rate is 2 °C min^{-1}. The insert is a zoom of the low temperature area.

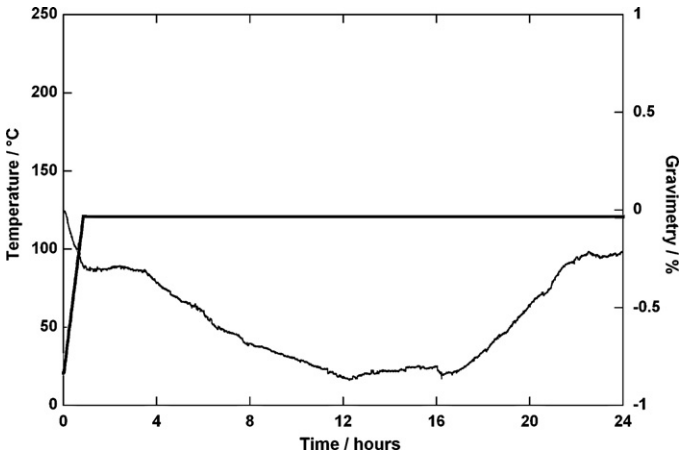

Fig. 5. TGA curve of an atmosphere preserved $LiFePO_4$–C sample during a 24 h at 120 °C stage in ambient atmosphere.

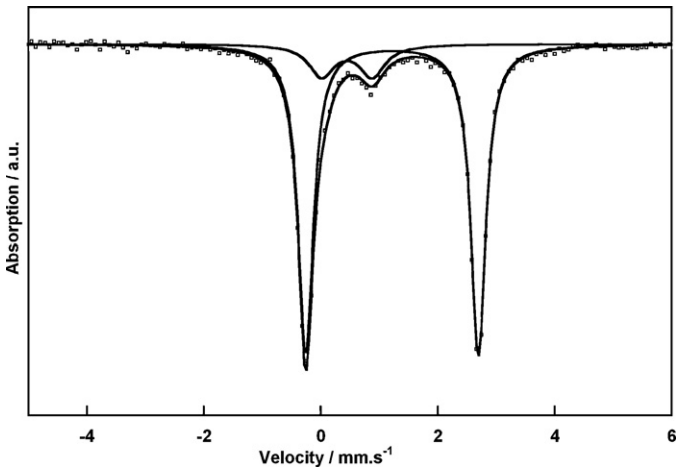

Fig. 7. Mössbauer spectrum of a $LiFePO_4$–C sample stored 10 days at 120 °C in ambient atmosphere.

reaction under dry air leads to a very regular increasing of mass in the 100–250 °C range with respect to the reaction under wet ambient air. This result shows that the reactivity at low temperature is influenced by the presence of water. Nevertheless, regarding the temperature of the beginning of oxidation in the case of dry air (around 160 °C), the oxygen alone induces some reactivity as well at moderate temperature. This is consistent with the results obtained previously [16], showing that dry air induces slight changes in the olivine structure even though water is not present.

In addition, to address the role of water in the reaction, a sample preliminary stored in argon has been exposed at 120 °C for 24 h in ambient atmosphere (Fig. 5). The corresponding TGA curve exhibits two well separated domains: during the first 12 h, the mass of the sample decreases by 0.8 wt%. This phenomenon can be attributed to the physisorbed-water due to sample preparation. After this first step and during the 12 following hours, the mass of the sample increases until it reaches approximately its initial mass. Previously published work by our group has proven that exposition of $LiFePO_4$ to ambient atmosphere at 120 °C leads to strong alteration [16] of the olivine structure along formation of amorphous ferric iron phosphate [20]. Most probably, adsorbed water loss and alteration of the material occur at the same time and only the balance of gain/loss is seen. In parallel, for a similar treatment in dry O_2 (Fig. 6), the sample mass undergoes only a slight increase in 27 h representing 0.15 wt%. This reaction is attributed to the oxidation of Fe(II) to Fe(III) along an oxygen uptake of the material, considering a direct reaction of O_2 with $LiFePO_4$. Nevertheless, a reaction with O_2 only cannot explain the 11% of trivalent iron observed by Mössbauer after 1 day storage at 120 °C in atmosphere [16]. Indeed, with one oxygen atom uptake for two oxidized Fe, the corresponding calculated percentage of trivalent iron would be 3% after 1 day in ambient atmosphere at 120 °C. Moreover, when 1% of relative humidity is introduced (Fig. 6) a 0.95 wt% mass uptake is observed in 24 h. Based on Eq. (2), the calculated corresponding percentage of trivalent iron would be 9.5% of oxidized iron which is consistent with the 12% observed previously by Mössbauer [16]. Considering the 3% Fe(III) corresponding to exposure to dry atmosphere, these results demonstrate clearly that although reaction with O_2 is occurring, the main cause of the alteration of $LiFePO_4$ is the reaction involving humidity contained in the atmosphere.

3.2. Structural and physico-chemical analyses

In order to ease the characterization of the changes, the conditions of storage have been aggravated with respect to previous work [16] by increasing the storage duration up to 10 days at 120 °C in ambient atmosphere. The Mössbauer spectrum displayed in Fig. 7 allows the quantification of the different Fe oxidation states in the corresponding aged sample. The spectrum mainly exhibits the Fe(II) doublet of $LiFePO_4$ with QS = 2.92 mm s^{-1} and IS = 1.21 mm s^{-1}. As it was already observed for softer atmosphere storage conditions, a doublet attributed to Fe(III) sites is also present. The deduced amount of trivalent iron represent 35% of the total iron content, which are three times the quantities found after only 1 day at 120 °C in ambient atmosphere [16] and significantly less than the amount found after 30 days at 120 °C

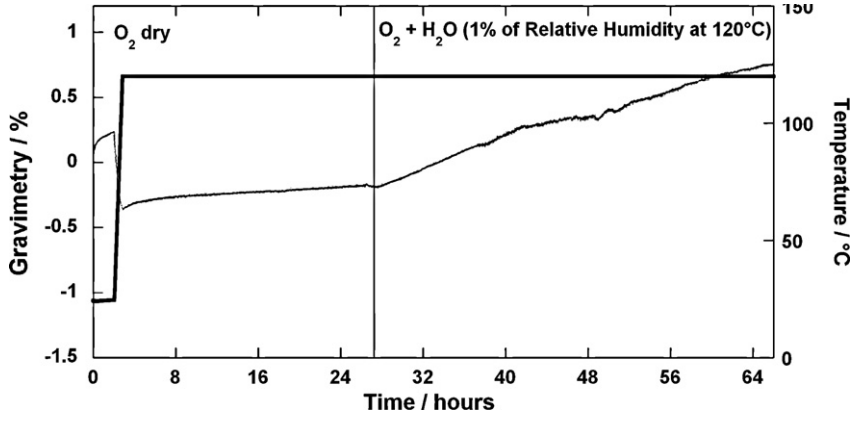

Fig. 6. TGA curve of an atmosphere preserved $LiFePO_4$–C sample during a 24 h 120 °C stage in dry O_2 followed by a stage in a wet atmosphere.

Table 2
Results obtained for $LiFePO_4$–C sample stored 10 days at 120 °C in ambient atmosphere via a quadrupolar splitting distribution fit.

Site	Average QS ($mm\,s^{-1}$)	QS distribution ($mm\,s^{-1}$)	FWHH ($mm\,s^{-1}$)	IS ($mm\,s^{-1}$)	(%)	
1	2.92	2.57–3.00	0.25	1.21	65	Fe(II)
2	0.90	0.25–1.30	0.40	0.44	35	Fe(III)

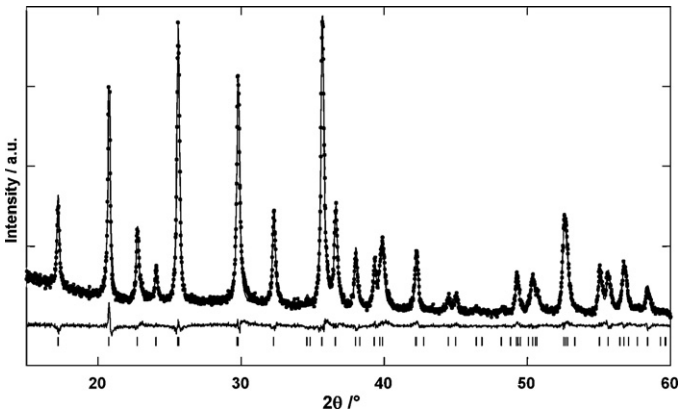

Fig. 8. XRD diagram of a $LiFePO_4$–C composite stored in atmosphere during 10 days at 120 °C.

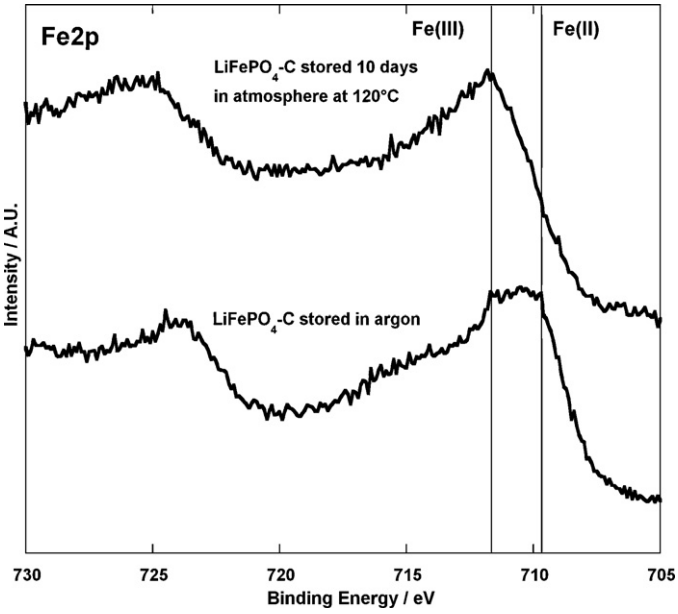

Fig. 9. Fe2p XPS spectrum of $LiFePO_4$–C preserved from atmosphere and exposed to atmosphere 10 days at 120 °C.

(45%) [20]. The significant amount of Fe(III) allowed to obtain accurate data about the corresponding site: QS = 0.90 $mm\,s^{-1}$ and IS = 0.44 $mm\,s^{-1}$ (Table 2). These values are in agreement with data previously found on this composite for a 1 day storage and 30 days storage at 120 °C in humid air and were previously assigned to an amorphous ferric phase formed along atmosphere exposure [20]. This result confirms that the reaction is only aggravated and does not lead to any new environment compared to a shorter treatment in similar conditions.

The XRD diagram of the 10 days aged sample, shown in Fig. 8, does not exhibit any additional crystalline phase other than the initial triphylite one. Moreover, the lattice parameters for the aged triphylite phase change when compared to those of a pristine, atmosphere preserved sample (Table 3). A significant decrease of *a* and *b* parameters and an increase of *c* is deduced from Rietveld refinement. This variation is expected for the departure of a small quantity of lithium from the triphylite phase in its solid solution domain [7,8]. Using Vegard's law, the corresponding lithium composition is $Li_{0.96}FePO_4$, which is within the "solid solution domain" limits of 80 nm $LiFePO_4$ particles ($Li_{0.96}FePO_4$ for 100 nm particles [7,9]) and so, does not lead to the formation of heterosite structure. The significant difference between the calculated quantity of lithium missing in the triphylite phase and the amount of Fe(III) visible via Mössbauer is attributed to the presence of the amorphous ferric phosphate phase. No evidence of cationic exchange could be found by Rietveld refinement as no increase of the lattice parameters values has been observed. Quantitative subsequent Rietveld refinements by adding an internal reference of crystallized Si in known amount prior aging, indicate that 15 wt% is amorphous, highly disordered or nano-crystallized. In addition, no Fe(III)-rich phase is visible to XRD in agreement with results previously published [20] in the case of a more severe aging treatment, confirming the formation upon air exposure of an amorphous ferric phosphate side phase, detrimentally to olivine $LiFePO_4$.

The new amorphous ferric phosphate phase due to aging in contact of ambient atmosphere, is expected to be present at the surface of the grains. For this reason, XPS has been used to monitor the evolution of the surface along the aging process over 10 days at 120 °C. The corresponding Fe2p XPS spectra are given in Fig. 9. The pristine sample exhibits a predominant signal of Fe(II) atoms at 709.8 eV whereas the surface of the aged sample seems mostly composed of a Fe(III)-rich phase visible at 711.8 eV. Indeed, the Fe(III)/Fe(II) ratio of the surface (around 10 nm deep) given by the quantification evolves from 0.7 to 4.8 for pristine to aged samples. (*Note*: the presence of small amounts of Fe(III) on a preserved sample may be due to unavoidable glove box pollution). This result allows concluding about the presence of a Fe(III)-rich surface of the particle. The visible olivine bonds have not evolved (Table 4). The characteristic phosphate peaks of P (P2p3/2 at 133.5 eV) and O (531.5 eV) are unchanged, indicating that phosphate groups are certainly preserved. No Fe–O bonds related to iron oxides can be seen on O1s region at 530 eV (see Fig. 10a). This proves the non-existence of iron oxides, such as Fe_2O_3, at the surface of our sample, consistent with Mössbauer results. In addition, there is no evidence, from the P2p data, of Li_3PO_4 that would be the counterpart of Fe_2O_3. Fe/P and $P/O_{phosphate}$ relative ratios are constant, indicating that the triphylite Fe/P/O stoichiometry is globally kept on the surface after the atmospheric alteration, supporting the presence of an iron phosphate at the surface of the particles. Although the Li1s signals cannot be separated from the Fe3p peaks, no carbonate Li_2CO_3

Table 3
Lattice parameters and crystallized phase quantification extracted from Rietveld refinement of the XRD diagrams obtained for $LiFePO_4$–C samples preserved from atmosphere and exposed to atmosphere 10 days at 120 °C. *x* gives the calculated equivalent missing lithium using a Vegard's law (see Ref. [16]).

Atmosphere treatment	*a* (Å)	*b* (Å)	*c* (Å)	*V* (Å^3)	*x*	Cryst. (%)
No exposure (R_{exp}: 2.08%, R_{wp}: 2.25%, R_p: 1.8%, GOF: 1.09, R_{bragg}: 0.521%)	10.3308(2)	6.0081(1)	4.6944(1)	291.378(6)	0	
Exposure 10 days 120 °C (R_{exp}: 2.51%, R_{wp}: 3.13%, R_p: 2.27%, GOF: 1.23, R_{bragg}: 0.651%)	10.3100(2)	5.9987(2)	4.6973(2)	290.51(1)	0.041	75(3)

Table 4
Results of XPS spectra analyses with core level peaks binding energies and atomic percentage. Fe2p3/2 "shake up" peaks have been taken into account for iron quantification.

Elements	No atmosphere exposure	Atmosphere exposure 10 days at 120 °C
C1s	284.6 eV (47%)	284.6 eV (46%)
	286.1 eV (4%)	285.9 eV (11%)
O1s	531.6 eV (34%)	531.4 eV (28%)
	–	533.1 eV (3%)
P2p3/2	133.6 eV (10%)	133.4 eV (8%)
Fe2p3/2	709.9 eV (3%)	709.8 eV (1%)
	711.8 eV (2%)	711.5 eV (3%)

characteristic peak (C1s at 290 eV) is visible (Fig. 10b), in agreement with Herstedt et al. [13] results and no peak corresponding to Li_2O at 528.3 eV on the O1s region is visible here. However, it is not possible to rule out the presence of LiOH.

Recent works done on different cathode materials using ^{7}Li MAS NMR have permitted to observe the presence of diamagnetic lithium compounds formed at the surface of paramagnetic materials [26–28]. The procedure of this analysis is extensively described elsewhere [28] and allows observing selectively ^{7}Li nuclei in an intrinsically diamagnetic phase on the surface of a paramagnetic electrode material. The ^{7}Li MAS NMR spectra obtained on a preserved sample and on a sample exposed to atmosphere 10 days at 120 °C are presented in Fig. 11. No quantifiable signal is obtained for both samples. Additionally, an experiment has been carried out by adding 4 wt% of LiOH (corresponding to the expected mass of LiOH that could be formed by 37% of lithium extraction from the triphylite), thoroughly mixed by mortar to an $LiFePO_4$–C sample in order to evaluate the signal due to such a quantity of lithium hydroxide intimately mixed with the paramagnetic $LiFePO_4$ phase. In that case, a signal is clearly observed near 0 ppm and displays a broad line shape characteristic of the interaction between LiOH and the surface of the $LiFePO_4$ grains. This suggests that most of the lithium localized on the surface is either present within the Fe(III)-rich surface phase or under the form of LiOH clusters "diluted" in the ferric phase and therefore in close intimacy with the paramagnetic active material, making the lithium signal not observable under a relatively high magnetic field (11.8 T).

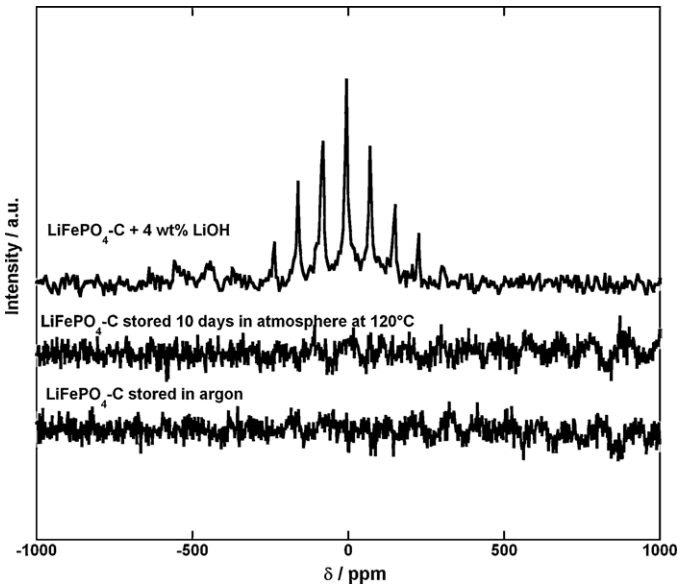

Fig. 11. ^{7}Li NMR spectra of $LiFePO_4$–C preserved from atmosphere, exposed to atmosphere 10 days at 120 °C and with the addition of 4 wt% of LiOH.

3.3. Electrochemical analyses

The electrochemical cycling (C/20) of a sample of $LiFePO_4$–C having been exposed to atmosphere 10 days at 120 °C is displayed in Fig. 12. In our previous work [16], a capacity gap has been observed between the first charge and the first discharge of a battery for a $LiFePO_4$–C cathode that was exposed to atmosphere 1 day at 120 °C. This phenomenon, proof of missing lithium ions in $LiFePO_4$ was in agreement with lithium extraction deduced from Rietveld refinements for a short aging time (i.e. 1 day at 120 °C). Nevertheless, in the case of the present 10 days-aged sample, the values of missing

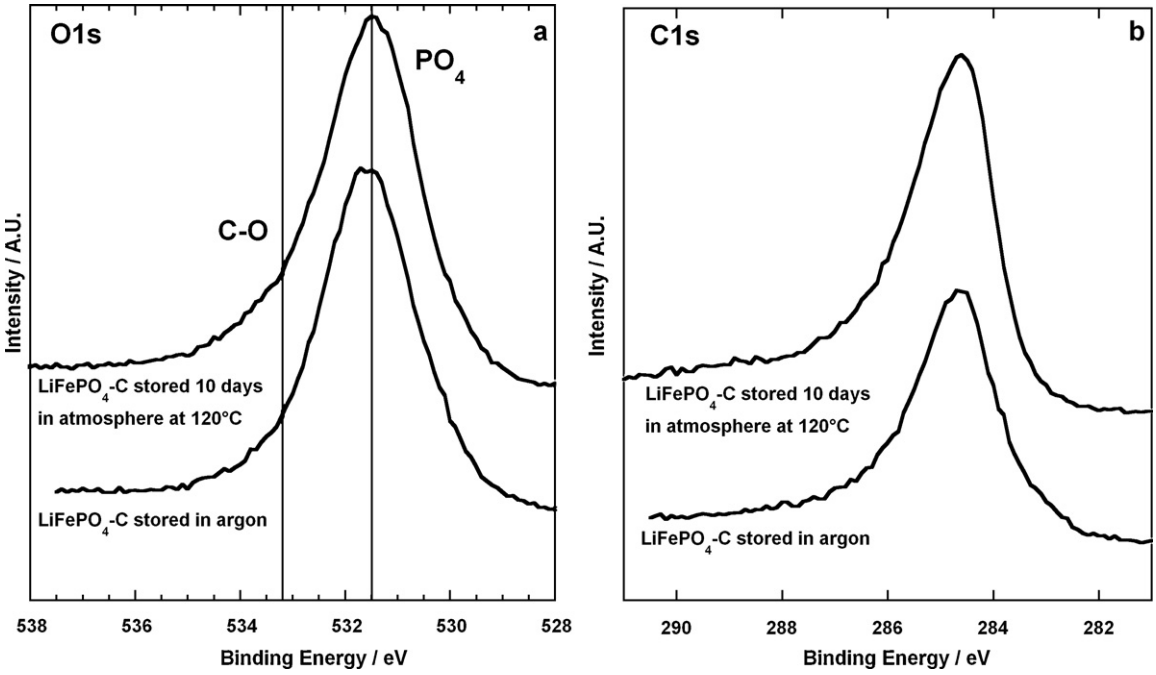

Fig. 10. O1s (a) and C1s (b) XPS spectrum of $LiFePO_4$–C preserved from atmosphere and exposed to atmosphere 10 days at 120 °C.

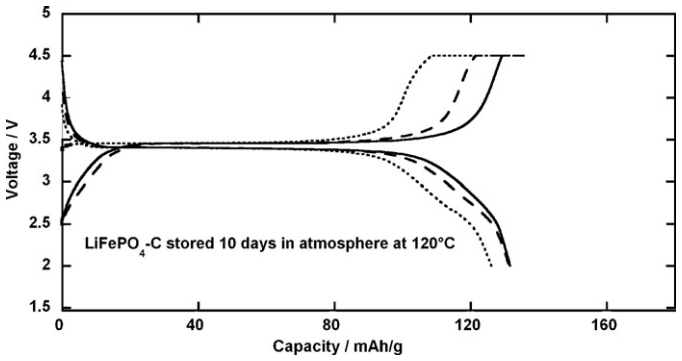

Fig. 12. First (dots), second (dashes) and fifth (line) galvanostatic cycles (discharge done at C/20 and charge done at CC/CV until C/200) of $LiFePO_4$–C exposed 10 days at 120 °C.

lithium (0.2 Li per formula unit) obtained from the capacity gap at the end of the first charge, with respect to the theoretical capacity, fit neither the high Fe(III) proportion given by Mössbauer (35%) nor the values of extracted lithium given via the Vegard's law (0.041 Li). Moreover, both the 2.6 V electrochemical process [20,29] and a strong capacity loss [19,20] (20% of the theoretical capacity) are visible mainly during the first discharge. This phenomenon already visible on the galvanostatic cycling of a sample exposed to atmosphere 1 day at 120 °C [16] is not observed on that of a preserved sample. This phenomenon is aggravated in the case of a sample aged for 30 days at 120 °C [20]. The capacity corresponding to the 2.6 V process at low voltage and the percentage of initial Fe(III) increase with the time of exposure to hot humid atmosphere. As a matter of fact, the specific capacity measured in the 3–2 V during the first discharge increases from 21 to 38 mAh/g along with the percentage of iron in the amorphous phase, from 31 to 38% for the samples exposed to atmosphere at 120 °C for 10 and 30 days respectively. The 2.6 V process and the percentage of Fe(III) are therefore linked together and can be now attributed to a consequence of the aging in atmosphere and not an intrinsic phenomenon of $LiFePO_4$, as it was proposed by Yu et al. [17].

The evolution of complex impedance spectra for 1 and 10 days aged samples after 1 complete electrochemical cycle is given in Fig. 13. The initial state of a 10 days aged sample is not very different from the initial state of a sample exposed only 1 day at 120 °C to atmosphere. A single semi-circle is visible, displaying a resistance of around 40–50 ohms before the Warburg diffusion and has been previously assigned to a charge transfer-double layer phenomenon [16]. After one entire galvanostatic cycle, a second phenomenon appears at lower frequencies, displaying a much higher resistance value. The significant expansion of the global resistance of the cathode appears to be linked to the poor specific capacity obtained for this sample. Its appearance after one galvanostatic cycle may be the sign of the transformation of this phase during the intercalation–deintercalation process and would be consistent with the presence of a Fe(III)-rich disordered phase forming a resistive shell around $LiFePO_4$ and leading to a new interface.

4. Discussion

Changes of olivine during its exposure to atmosphere are expected to be the consequence of a superficial oxidation. We demonstrated in particular, that water is an essential element of the reactivity of olivine in ambient atmosphere. To summarize the characterization analyses, it has been shown that the crystallographic cell of our $LiFePO_4$–C sample exposed 10 days at 120 °C to ambient atmosphere undergoes a volume shrinking that can be linked to the departure of Li from the structure with a

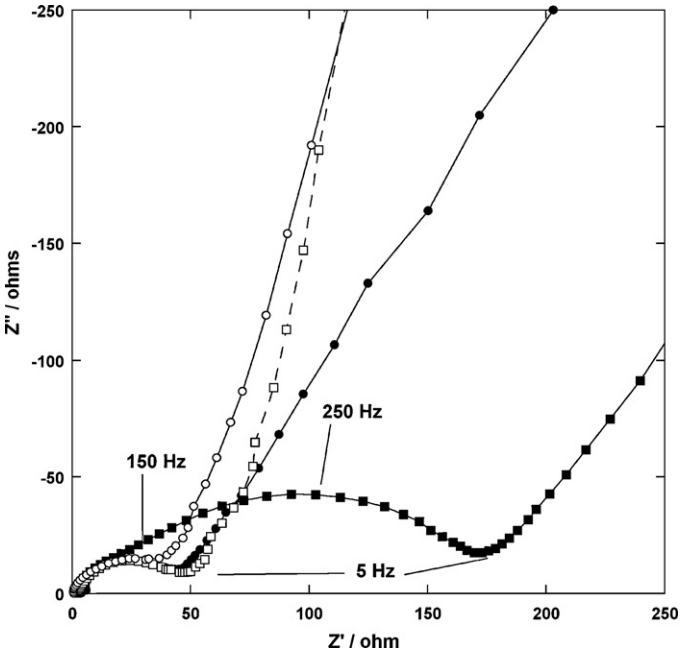

Fig. 13. Impedance spectra obtained for $LiFePO_4$–C exposed to atmosphere 1 day at 120 °C (white symbols) and 10 days at 120 °C (filled symbols), in the initial state (dots) and fully reduced state after 1 cycle (square).

migration most certainly to the surface of the particles. The cell volume decreases when the exposure time increases. This change is observed in parallel with the oxidation of the iron atoms situated on the surface of the olivine. Masquelier and co-workers [19] linked the lattice volume decrease observed at 150 °C to the migration of iron from the core to the surface creating vacancies in the centre of the particle yielding $(Li_{1-\varepsilon-x}Fe_y)_{M1}(Fe_{1-y-\varepsilon'}Li_x)_{M2}PO_4$. Nevertheless, the migration of iron atoms from the core toward the surface of $LiFePO_4$ particles induces the presence of excess of iron which should oxidize at the particle surface to form a significant amount of Fe_2O_3. However, in the work presented here, for milder temperature conditions, neither XRD nor Mössbauer give any evidence of the formation of such oxide for heat treatments at 120 °C for 10 days or 30 days [20]. In addition, such a significant amount of Fe(III) is not found in the diffracting part of the particle, and therefore is probably present in an amorphous phase, on the surface of particles as confirmed by the high Fe(III)/Fe(II) ratio obtained from XPS. Without any evolution of the Fe/P ratio found by XPS and supported by Mössbauer results, the Fe(III) can be considered in a phosphate environment.

The lattice shrinking, occurring in the bulk is the sign of the creation of Li vacancies, within the solid solution domain, in the structure of olivine $LiFePO_4$. The most probable two defects appear-

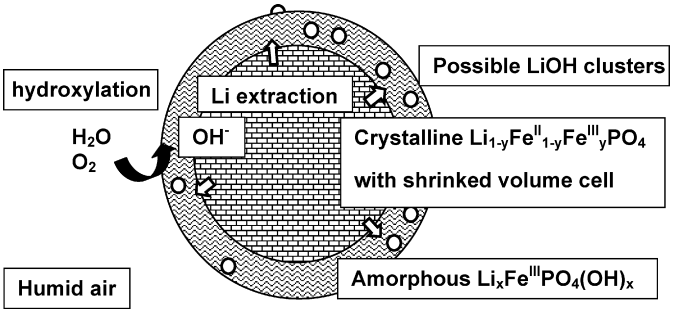

Fig. 14. Overview of the consequences of atmosphere exposure of olivine $LiFePO_4$ at 120 °C.

ing in such structure under soft conditions of temperature are antisites and lithium vacancies, as demonstrated by Islam and coworkers [30]. Nevertheless, no evidence of cationic exchange could be found by Rietveld refinement as no increase of the lattice parameters values has been observed. Such deintercalation of lithium from $LiFePO_4$ is not contradicted by our present results as Li still can be near the surface as LiOH in great intimacy with iron-containing phases and not observable by NMR or as lithium excess present in the superficial amorphous phase. Previous combined TGA and mass spectroscopy [20] indicated the departure of water for an aged sample heated up to 450 °C under argon. From this study, a $Li_xFe^{III}PO_4(OH)_x$ formula was proposed for the amorphous phase resulting from the aging process to fit at the same time the departure of lithium, hydration rate and the presence of solely ferric iron. The $Li_xFePO_4(OH)_x$ formula of the surface ferric phosphate phase, as proposed in Ref. [20] and consistent with results developed in this work is lithium deficient, and therefore cannot contain the excess lithium due to the deintercalation of the $LiFePO_4$ crystalline phase. Consequently, the presence of small LiOH clusters in strong interaction with the paramagnetic Fe, which would make them undetectable by NMR seems to be the most reasonable interpretation.

It seems then reasonable, considering a role of both oxygen and water to propose the following mechanism:

$$LiFe^{II}PO_4 + 1/2H_2O + 1/4O_2 \Rightarrow Li_xFe^{III}{}_xPO_4(OH)_x + (1-x)LiOH \quad (4)$$

Fig. 14 summarizes the possible overall changes that could explain our results, in agreement with results previously obtained in [20].

5. Conclusion

The study of a $LiFePO_4$–C sample having undergone a stay of 10 days at 120 °C under ambient atmosphere has been carried out to shed a light on its degradation process at moderate temperature (below 150 °C). TGA results showed the determinant role of water in this process, indicating that the aging process in ambient atmosphere is more complicated than a simple oxidation. The appearing of a disordered ferric phosphate phase is observed on the surface of particles, keeping the $FePO_4$ stoichiometry and, in parallel, the lithium extraction, is responsible for a cell volume shrinking in the core. No Fe_2O_3 can be observed by Mössbauer proving the particular effect of moderate temperature (below 150 °C) atmosphere exposure compared to higher temperature. Concerning lithium, the atoms extracted from the core are most probably under the form of LiOH clusters in close intimacy with paramagnetic iron phase. The presence of the surface $Li_xFePO_4(OH)_x$ disordered phase, able to intercalate lithium with a bad reversibility around 2.6 V, leads to an increase of the electrode resistance and to the degradation of the electrochemical performance. An important result is that the storage conditions used for this material must be drastically set to avoid any alteration of the phase, even at low temperature. Based on these results and previously published data on samples aged at room temperature [16], most probably the same aging mechanism apply to sample stored in ambient atmosphere at room temperature.

Acknowledgements

The authors wish to thank Dr. Danielle Gonbeau and Dr. Remi Dedryvère for helpful discussion on XPS analysis and Dr. Alain Wattiaux for Mössbauer experiments. Financial support of the Ph.D. of Jean Frédéric Martin from the Region Pays de la Loire is gratefully acknowledged.

References

[1] A.K. Padhi, K.S. Nanjundaswamy, J.B. Goodenough, J. Electrochem. Soc. 144 (1997) 1188.
[2] H. Huang, S.C. Yin, L.F. Nazar, Electrochem. Solid-State Lett. 4 (2001) A170.
[3] C.H. Mi, G.S. Cao, X.B. Zhao, Mater. Lett. 59 (2005) 127.
[4] R. Dominko, M. Bele, M. Gaberscek, M. Remskar, D. Hanzel, S. Pejovnik, J. Jamnik, J. Electrochem. Soc. 152 (2005) A607.
[5] A. Yamada, S.C. Chung, K. Hinokuma, J. Electrochem. Soc. 148 (2001) A224.
[6] K. Kanamura, S. Koizumi, K. Dokko, J. Mat. Sci. 43 (2008) 2138.
[7] A. Yamada, H. Koizumi, N. Sonoyama, R. Kanno, Electrochem. Solid-State Lett. 8 (2005) A409.
[8] A. Yamada, H. Koizumi, S. Nishimura, N. Sonoyama, R. Kanno, M. Yonemura, T. Nakamura, Y. Kobayashi, Nat. Mater. 5 (2006) 357.
[9] L. Laffont, C. Delacourt, P. Gibot, M.Y. Wu, P. Kooyman, C. Masquelier, J.M. Tarascon, Chem. Mater. 18 (2006) 5520.
[10] M. Ménétrier, C. Delmas, L. Croguennec, F. Le Cras, F. Weill, Nat. Mater. 7 (2008) 665.
[11] N. Meethong, H.-Y.S. Huang, W.C. Carter, Y.-M. Chiang, Electrochem. Solid-State Lett. 10 (2007) A134.
[12] N. Meethong, H.Y.S. Huang, S.A. Speakman, W.C. Carter, Y.M. Chiang, Adv. Funct. Mater. 17 (2007) 1115.
[13] M. Herstedt, M. Stjerndahl, A. Nyten, T. Gustafsson, H. Rensmo, H. Siegbahn, N. Ravet, M. Armand, J.O. Thomas, K. Edström, Electrochem. Solid-State Lett. 6 (9) (2003) A202.
[14] Y.-H. Rho, L.F. Nazar, L. Perry, D. Ryan, J. Electrochem. Soc. 154 (4) (2007) A283.
[15] A. Yamada, H. Koizumi, S.-I. Nishimura, N. Sonoyama, R. Kanno, M. Yonemura, T. Nakamura, Y. Kobayashi, Nat. Mater. 5 (2006) 357.
[16] J.-F. Martin, A. Yamada, G. Kobayashi, S. Nishimura, N. Dupré, R. Kanno, D. Guyomard, Electrochem. Solid-State Lett. 11 (2008) A12.
[17] D.Y.W. Yu, K. Donoue, T. Kadohata, T. Murata, S. Matsuta, S. Fujitani, J. Electrochem. Soc. 155 (2008) A526.
[18] G. Kobayashi, S. Nishimura, M. Park, R. Kanno, M. Yashima, T. Ida, A. Yamada, Adv. Funct. Mater. 19 (2009) 395.
[19] S. Hamelet, P. Gibot, M. Casas-Cabanas, D. Bonnin, C.P. Grey, J. Cabana, J.B. Leriche, J. Rodriguez-Carvajal, M. Courty, S. Levasseur, C. Masquelier, J. Mater. Chem. 19 (23) (2009) 3979.
[20] M. Cuisinier, J.-F. Martin, N. Dupré, A. Yamada, R. Kanno, D. Guyomard, Electrochem. Commun. 12 (2) (2010) 238.
[21] P. Keller, A.M. Fransolet, F. Fontan, Contrib. Mineral. Petrol. 92 (1986) 502.
[22] F. Hatert, P. Schmid-Beurmann, Fe2+ oxidation in triphylite LiFePO4: possible formation of Ferrisicklerite and Heterosite, in: European Conference on Mineralogy, E. Schweizerbart Science Publishers, 2005.
[23] P.B. Moore, Pegmatite Minerals of P(V) and B(III), Mineralogical association of Canada, 1985.
[24] A.M. Fransolet, in: Granitic Pegmatites: the state of the art—International Symposium 06th, Porto, 2007.
[25] K. Edström, T. Gustafsson, J.O. Thomas, Electrochim. Acta 50 (2004) 397.
[26] M. Ménétrier, C. Vaysse, L. Croguennec, C. Delmas, C. Jordy, F. Bonhomme, P. Biensan, Electrochem, Solid State Lett. 7 (6) (2004) A140.
[27] N. Dupré, J.-F. Martin, J. Oliveri, J. Degryse, D. Guyomard, Ionics 14 (2008) 203.
[28] N. Dupré, J.-F. Martin, J. Oliveri, P. Soudan, D. Guyomard, A. Yamada, R. Kanno, J. Mater. Chem. 18 (2008) 4266.
[29] N. Marx, L. Croguennec, D. Carlier, L. Bourgeois, P. Kubiak, F. Le Cras, C. Delmas, Chem. Mater. 22 (5) (2010) 1854.
[30] C.A.J. Fisher, V.M. Hart Prieto, M.S. Islam, Chem. Mater. 20 (2008) 5907.